



Physical and electrochemical properties of LiCoPO₄/C nanocomposites prepared by a combination of emulsion drip combustion and wet ball-milling followed by heat treatment

Renat Tussupbayev, Izumi Taniguchi*

Department of Chemical Engineering, Graduate School of Science and Engineering, Tokyo Institute of Technology, 12-1, Ookayama-2, Meguro-ku, Tokyo 152-8552, Japan

HIGHLIGHTS

- ▶ LiCoPO₄/C nanocomposites could be prepared by a novel preparation route.
- ▶ They consisted of the agglomerates of LiCoPO₄ primary particles.
- ▶ A thin layer of amorphous carbon was formed on the LiCoPO₄ primary particles.
- ▶ The nanocomposite cathode delivered an energy density of 595 Wh kg^{−1} at 0.1 C.
- ▶ The capacity retention is 87% after 25 cycles at 0.1 C.

ARTICLE INFO

Article history:

Received 1 October 2012

Received in revised form

28 December 2012

Accepted 13 January 2013

Available online 20 February 2013

Keywords:

Emulsion drip combustion

Fluidized bed reactor

Lithium cobalt phosphate

Cathode

Lithium ion batteries

ABSTRACT

The combination of emulsion drip combustion at 600 °C and wet ball-milling followed by heat treatment at 500 °C in a N₂ + 3% H₂ atmosphere was performed for the preparation of LiCoPO₄/C nanocomposites. The obtained material consisted of agglomerates of LiCoPO₄ primary particles with a geometric mean diameter of 70 nm, which were covered by a thick layer of amorphous carbon. A cell containing the LiCoPO₄/C nanocomposites exhibited a discharge capacity of 134 mAh g^{−1} at a charge-discharge rate of 0.1 C. However, the discharge profile of the LiCoPO₄/C nanocomposites had a long tail, which may be due to the limited lithium ion diffusion caused by the thick carbon layer that formed on the LiCoPO₄ primary particles. The LiCoPO₄/C nanocomposites prepared from a mixture of kerosene and heptane with equal volumes consisted of agglomerates of the primary particles with a geometric mean diameter of 97 nm, which were covered by a thin layer of amorphous carbon with a thickness on the order of 10 nm. Furthermore, they delivered a high energy density of 595 Wh kg^{−1} at a charge-discharge rate of 0.1 C and exhibited reasonable cyclability, retaining 87% of the initial energy density after 25 cycles.

© 2013 Elsevier B.V. All rights reserved.

1. Introduction

Since Padhi et al. [1] first proposed the use of olivine-structured LiMPO₄ (M = Fe, Mn, Co and Ni) as cathodes for Li-ion batteries in 1997, they have been widely investigated for use as substitute commercial LiCoO₂ cathodes. Later, Amine et al. [2] showed the possibility of reversibly extracting lithium ions from olivine LiCoPO₄. This material has attracted the attention of researchers because of its high operating potential of 4.8 V vs. Li⁺/Li and high

theoretical capacity of 167 mAh g^{−1}. These properties enable LiCoPO₄ to deliver a specific energy density as large as 750 Wh kg^{−1}. However, it has low electronic conductivity (<10^{−9} S cm^{−1}), which limits its practical use as a cathode for Li-ion batteries [3,4]. Several methods have been applied to overcome this drawback and improve the electrochemical performance of LiCoPO₄, such as the reduction in particle size [5,6] and doping with Fe, Ni or V cations [7–10]. Moreover, coating LiCoPO₄ particles with thin layers of Al₂O₃ or LiFePO₄ can greatly alleviate capacity fading [11,12]. The preparation of LiCoPO₄/C (carbon) composite materials is a common method for improving the electrochemical properties of olivine compounds [13,14].

Thus far, the preparation of LiCoPO₄/C composites has been performed by conventional synthetic methods, such as a solid-state

* Corresponding author. Tel./fax: +81 3 5734 2155.

E-mail addresses: taniguchi.iaa@m.titech.ac.jp, itaniguc@chemeng.titech.ac.jp (I. Taniguchi).

reaction [14], mechanochemical activation [9], microwave heating [15], hydrothermal synthesis [16,17], precipitation [18], the sol–gel method [19] and a solvothermal process [20]. As a result, the use of LiCoPO₄/C nanocomposites appears to be a promising means of solving this problem because the well-dispersed conductive carbon on the LiCoPO₄ nanoparticles provides an effective pathway for electron and lithium ion transport. However, the above techniques have several disadvantages, such as a heterogeneous composition, a long annealing time at a high temperature, a complex preparation route or a low yield of the lithium component. Few simple and convenient processing approaches have been reported for LiCoPO₄/C nanocomposites that are feasible for industrial application. Thus, we have developed a novel and simple technique for the preparation of LiCoPO₄/C nanocomposites from emulsion droplets using a combination of drip combustion in a fluidized bed reactor and wet ball-milling followed by heat treatment. Furthermore, the physical and electrochemical properties of the obtained materials have been investigated.

2. Experimental

2.1. Precursor solution

The precursor solution was prepared by dissolving a stoichiometric ratio of LiNO₃, Co(NO₃)₂·6H₂O and H₃PO₄ in distilled water. The total concentration of Li⁺, Co²⁺ and PO₄^{3−} in the water phase was 1.5 mol dm^{−3}. The precursor solution was mixed with a surfactant and one of three types of organic solvent: kerosene, heptane and a mixture of kerosene and heptane with a volume ratio of 50/50. The mixture was vigorously stirred by a homogenizer at a rotation speed of 5000 rpm for 10 min. The resulting emulsion with a fixed volume ratio of organic solvent to water (60:40) was used as the starting solution to synthesize LiCoPO₄/C.

2.2. Experimental setup and procedure

A schematic diagram of the experimental apparatus has been given elsewhere [21]. The apparatus consists of four main sections: a gas-flow control and measurement system, a fluidized bed reactor installed in three electric furnaces, a liquid-precursor feed supply and a particle collection system. The fluidized bed reactor is a cylindrical quartz glass tube with a 31.5 mm internal diameter and an 880 mm effective length. The three external electric furnaces, which were equipped with PID controllers, heated the reactor. Medium particles in the reactor were fluidized by using air supplied from the bottom of the reactor by a compressor through a rotameter and a filter. Spherical alumina particles with a geometric mean diameter of $d_{p,g} = 399 \mu\text{m}$ and a geometric standard deviation of $\sigma_g = 1.07$ were used as the medium particles. The starting solution was supplied to a stainless-steel nozzle (1 mm I.D. and 2 mm O.D.) by a peristaltic pump and then dripped from the tip of the nozzle. The nozzle was mounted at the top of the reactor and cooled by air from the compressor to prevent the nozzle from heating up. The emulsion droplets of the starting solution that form at the tip of the nozzle freely fall to the bottom of the reactor, collide with fluidized medium particles and divide into finer droplets. These droplets are then converted to solid particles in the reactor. Owing to the difference in the terminal velocity between the solid particles and medium particles, the solid particles are entrained from the reactor and collected using a cyclone and a bag filter. The synthesis was carried out at reactor temperatures $T = 400\text{--}800^\circ\text{C}$ and a fluidization number U_0 (superficial velocity)/ U_{mf} (minimum fluidized velocity) = 5. U_{mf} was calculated using the correlation of Wen and Yu [22] after

considering the effects of temperature on the density and viscosity of a gas.

The LiCoPO₄/C composites were prepared by an emulsion drip combustion followed by annealing at 500 °C in a N₂ + 3% H₂ atmosphere. On the other hand, the LiCoPO₄/C nanocomposites were prepared by a combination of emulsion drip combustion and wet ball-milling followed by annealing at 500 °C for 4 h in a N₂ + 3% H₂ atmosphere. In the wet ball-milling procedure, the rotation speed was 800 rpm and the ball-milling time was fixed at 3 h.

2.3. Physical characterization

The crystalline phase of the samples was identified by X-ray diffraction (XRD, Rigaku, Ultima IV with D/teX Ultra) analysis with Cu-K α radiation. The lattice parameters of the materials were refined by Rietveld analysis using the integrated X-ray powder diffraction software package PDXL (Rigaku, Version 1.3.0.0). The surface morphology of the samples was examined by field-emission scanning electron microscopy (FE-SEM, Hitachi, S-4500). The particle size distribution was determined by randomly sampling approximately 500 particles from the SEM images. The geometric mean diameter $d_{g,p}$ and geometric standard deviation σ_g were calculated using

$$\ln d_{g,p} = \sum \frac{\ln d_i}{N}, \quad (1)$$

$$\ln \sigma_g = \left[\frac{\sum (\ln d_i - \ln d_{g,p})^2}{N - 1} \right]^{1/2}, \quad (2)$$

respectively, where N is the total number of samples. The interior structure of the samples was observed using a transmission electron microscopy (TEM) system (JEOL Ltd., JEM-2010F) capable of energy-dispersive spectroscopy (EDS) and selected-area electron diffraction (SAED).

The specific surface area was determined by the Brunauer–Emmett–Teller method (BET, Shimadzu Co., Flow Sorb II 2300). The carbon content was measured using an element analyzer (CHN Corder MT-6, YANACO).

2.4. Electrochemical characterization

Electrochemical characterization was performed by assembling a CR2032 coin cell for galvanostatic charge–discharge testing. The cell comprised a lithium metal negative electrode and a LiCoPO₄/C composite positive electrode separated by a microporous polypropylene film. A 1 mol dm^{−3} solution of LiPF₆ in a solvent of ethylene carbonate (EC) and dimethyl carbonate (DMC) with 1:1 volume ratio (Tomiya Pure Chemical Co., Ltd.) was used as the electrolyte. The cathode consisted of 70 wt.% LiCoPO₄/C, 10 wt.% polyvinylidene fluoride (PVDF) as a binder and 20 wt.% acetylene black. The cell was cycled galvanostatically between 2.5 and 5.1 V on multichannel battery testers (Hokuto Denko, HJ1010mSM8A) at various charge–discharge rates ranging from 0.1 to 2 C (1 C = 167 mAh g^{−1}). The current density and specific capacity were calculated on the basis of the mass of LiCoPO₄ in the cathode. Cyclic voltammetry (CV) and electrochemical impedance spectroscopy (EIS) measurements were performed with a Solartron SI 1287 electrochemical interface at a scanning rate of 0.1 mV s^{−1} and in the frequency range from 100 kHz to 0.1 Hz with an amplitude of 10 mV. All measurements were performed at room temperature.

3. Preparation of LiCoPO₄/C composites by emulsion drip combustion followed by heat treatment

3.1. Effect of synthesis temperature on physical properties of LiCoPO₄/C composites

Fig. 1 shows the XRD patterns of the samples synthesized by emulsion drip combustion in the fluidized bed reactor at synthesis temperatures from 400 to 800 °C. The JCPDS card pattern of LiCoPO₄ is also shown in the figure. The diffraction peaks of all the samples are identified as those of an orthorhombic olivine-type structure with the space group *Pnma*. However, some Li₃PO₄ impurity peaks are also detected.

In order to avoid the formation of Li₃PO₄ and improve the crystallinity of the as-prepared samples, the samples were annealed at 500 °C for 4 h in a N₂ + 3% H₂ atmosphere. Fig. 2 shows the XRD patterns of the as-annealed samples. For the samples prepared at 400 and 800 °C, the peak intensity of the Li₃PO₄ impurity phase was considerably less than that of the as-prepared samples. Moreover, the Li₃PO₄ phase completely disappeared after annealing the sample prepared at 600 °C. The physical properties of the as-annealed samples, such as the lattice parameters obtained by Rietveld refinement, the carbon content and the specific surface area, are summarized in Table 1. The refined lattice parameters for the samples prepared at temperatures from 400 to 800 °C are in good agreement with those reported by Amine et al. [2] and Lloris et al. [5]. The samples prepared at 400 and 600 °C had a similar carbon content, whereas the sample prepared at 800 °C had a larger carbon content of 66 wt.%. The specific surface area of these materials markedly increases with the synthesis temperature from 25 m² g^{−1} at a synthesis temperature of 400 °C to 65 m² g^{−1} at a synthesis temperature of 800 °C.

From the above results, it is concluded that LiCoPO₄/C composites are successfully synthesized by emulsion drip combustion at 600 °C in a fluidized bed reactor followed by annealing at 500 °C in a N₂ + 3% H₂ atmosphere.

3.2. Electrochemical properties of LiCoPO₄/C composites

Fig. 3 shows the initial discharge profiles of the LiCoPO₄/C composites synthesized at temperatures from 400 to 800 °C and then annealed at 500 °C in a N₂ + 3% H₂ atmosphere. The final LiCoPO₄/C composites synthesized at 400 °C have a potential

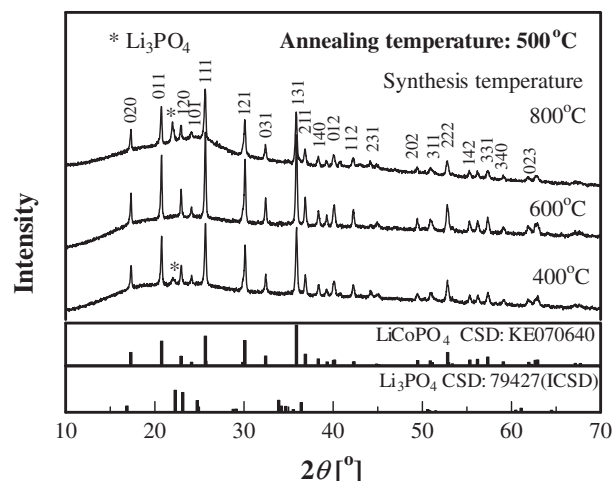


Fig. 2. XRD patterns of LiCoPO₄/C samples synthesized at temperatures from 400 to 800 °C and then annealed at 500 °C. Organic solvent: kerosene.

plateau at approximately 4.8 V vs. Li⁺/Li, and the potential rapidly declines, finally exhibiting a low discharge capacity of 82 mAh g^{−1}. This might be due to the low crystallinity of the material caused by the low synthesis temperature, as indicated by the XRD peak intensities. The LiCoPO₄/C composites prepared at 800 °C exhibit a larger discharge capacity of 115 mAh g^{−1} despite their lower crystallinity. However, the discharge profile has a long tail, indicating the high resistance of charge transfer in the cathode. This may be due to the limited lithium ion diffusion, resulting from the very high carbon content of about 66 wt.%. Although the addition of carbon increases the electronic conductivity in the cathode, a thick carbon layer may prevent the diffusion of lithium ion in the LiCoPO₄ particles. The LiCoPO₄/C composites synthesized at 600 °C exhibited an improved discharge curve with a prolonged potential plateau and a much shorter tail. However, the discharge capacity was 103 mAh g^{−1}, which corresponds to 62% of the theoretical capacity (167 mAh g^{−1}). This may be due to the larger particle size of LiCoPO₄ prepared by drip combustion in a fluidized bed reactor followed by heat treatment [21].

4. Preparation of LiCoPO₄/C nanocomposites by combination of emulsion drip combustion and wet ball-milling followed by heat treatment

4.1. Preparation of LiCoPO₄/C nanocomposites

Olivine compounds suffer from a low electronic conductivity; thus, reducing the distance of the lithium ion diffusion path is essential to improve of their electrochemical properties [23]. Therefore, in order to decrease the particle size of LiCoPO₄, the

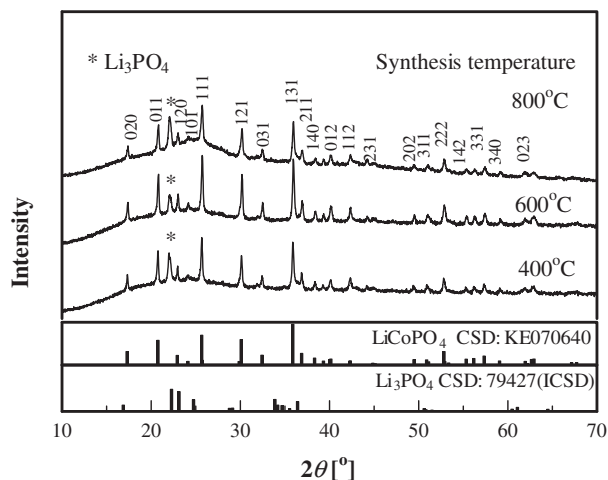


Fig. 1. XRD patterns of LiCoPO₄/C samples synthesized at temperatures from 400 to 800 °C. Organic solvent: kerosene.

Table 1

Lattice parameters, composition and specific surface area of LiCoPO₄/C samples prepared at different temperatures from 400 to 800 °C and then annealed 500 °C. Organic solvent: kerosene.

Sample	Lattice parameters			Carbon content [wt.%]	BET [m ² g ^{−1}]
	Synthesis temperature [°C]	Annealing temperature [°C]	<i>a</i> [Å] <i>b</i> [Å] <i>c</i> [Å]		
400	400	500	10.2052 5.9246 4.7024	35	25
600	600	500	10.2036 5.9236 4.7014	37	33
800	800	500	10.2070 5.9255 4.7039	66	65

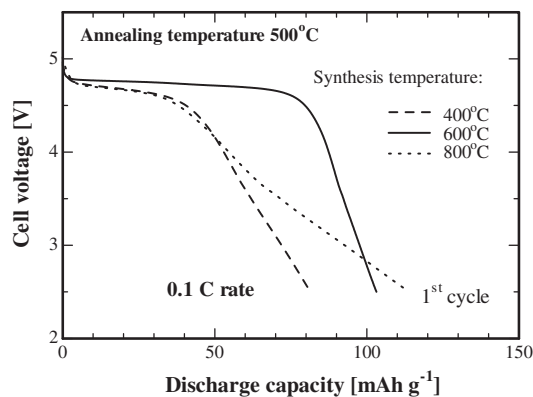


Fig. 3. First discharge curves of LiCoPO_4/C composites prepared at temperatures from 400 to 800 °C and then annealed at 500 °C. Organic solvent: kerosene.

LiCoPO_4/C composite sample synthesized at 600 °C was milled in ethanol by planetary ball-milling for 3 h at a rotation speed of 800 rpm, which was followed by annealing at 500 °C for 4 h in a $\text{N}_2 + 3\% \text{H}_2$ atmosphere.

Fig. 4 shows the XRD pattern of the obtained sample. The diffraction peaks of the sample are also identified as those of an orthorhombic olivine-type structure with the space group $Pnma$. The morphology of the sample was observed by SEM and the obtained images are displayed in Fig. 5. The primary particles are well dispersed and soft agglomerates were observed in the SEM images (Fig. 5a). Fig. 5b shows the particle size distribution of the sample. The geometric mean diameter $d_{g,p}$ and geometric standard deviation σ_g of the sample were 70 nm and 1.37, respectively. LiCoPO_4 primary particles with a uniform particle size distribution could be prepared by the present method. In order to clarify the internal structure of the sample, the sample was investigated by TEM, SAED and EDS, the results of which are displayed in Fig. 6. The EDS spectra exhibit the composition of the sample at the circled points on the magnified TEM image. The dark region in this image was identified as a LiCoPO_4 nanoparticle covered by carbon, while the surrounding layer consists of only carbon. Furthermore, the corresponding SAED patterns indicate the formation of crystallized LiCoPO_4 nanoparticles, as evidenced from the diffraction spots, as well as an amorphous carbon layer on the LiCoPO_4 nanoparticles indicated by the hollow ring. Thus, the LiCoPO_4/C nanocomposites were successfully prepared by the combination of emulsion drip combustion and wet ball-milling followed by heat treatment.

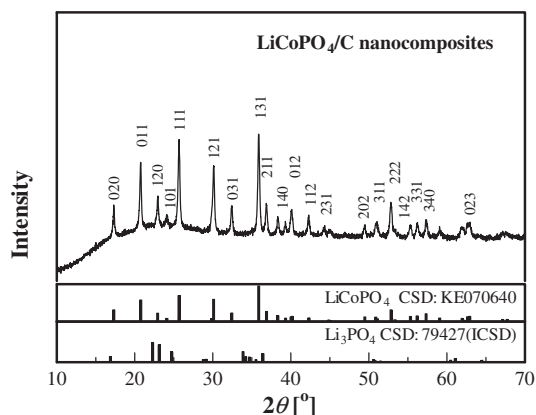


Fig. 4. XRD patterns of LiCoPO_4/C sample. Organic solvent: kerosene.

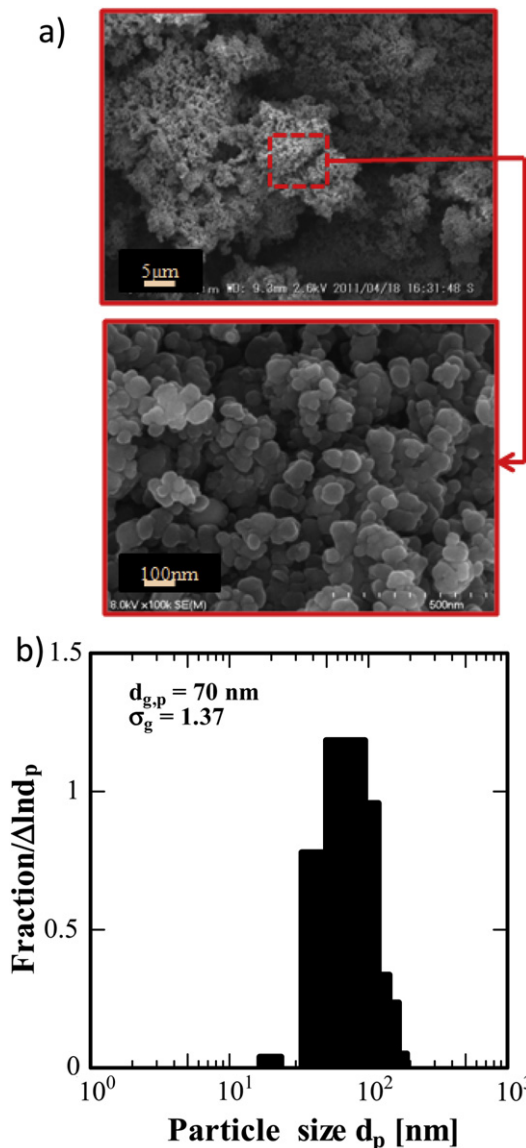


Fig. 5. SEM (a) and particle size distribution (b) of LiCoPO_4/C sample. Organic solvent: kerosene.

4.2. Electrochemical properties of LiCoPO_4/C nanocomposites

The initial discharge profile of the LiCoPO_4/C nanocomposites is shown in Fig. 7. For comparison, the initial discharge curve of the LiCoPO_4/C composites is also shown in the figure. Both materials exhibit similar discharge plateaus at approximately 4.8 V. The LiCoPO_4/C nanocomposites delivered a discharge capacity of 135 mAh g^{-1} , which corresponds to 80% of the theoretical capacity. The initial discharge capacity was increased from 103 to 135 mAh g^{-1} by the reduction of the LiCoPO_4 primary particle size. However, the discharge profile of the LiCoPO_4/C nanocomposites has a longer tail than that of the LiCoPO_4/C composites, which may be due to the limited lithium ion diffusion caused by the thick carbon layer that formed on the LiCoPO_4 particles, as shown in Fig. 6. A promising means of further improving the electrochemical properties of the LiCoPO_4/C nanocomposites may be to reduce their carbon content. The present synthesis process involves the carbonization of an organic solvent due to the incomplete combustion during emulsion drip combustion. Thus, we attempted to

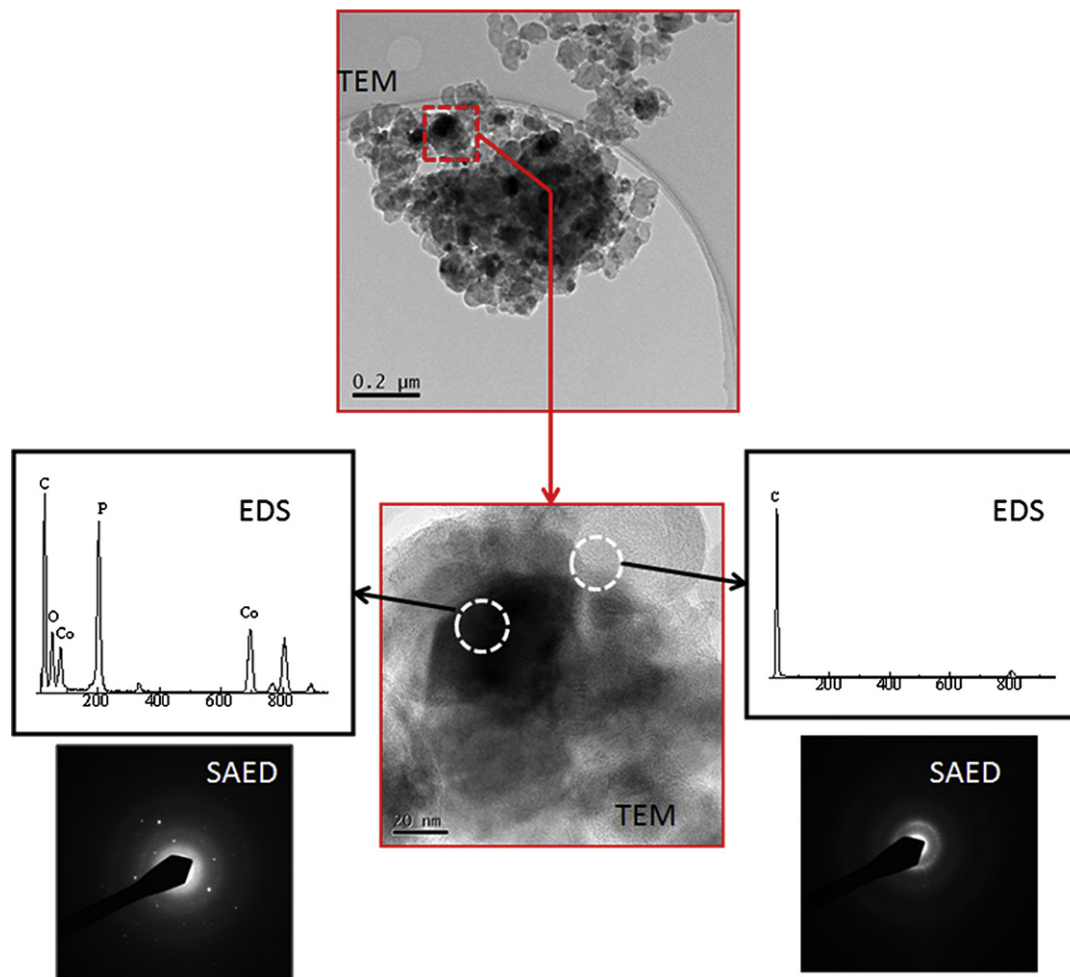


Fig. 6. TEM and SAED images with EDS spectra of LiCoPO_4/C nanocomposites. Organic solvent: kerosene.

decrease the carbon content by substituting kerosene for a lighter hydrocarbon such as pure heptane or a mixture of kerosene and heptane with a volume ratio of 50/50.

4.3. Electrochemical properties of LiCoPO_4/C nanocomposites obtained from different organic solvents in emulsion

Fig. 8 shows XRD patterns of the LiCoPO_4/C nanocomposite samples synthesized by the present method from different organic

solvents in emulsion: heptane, kerosene and a mixture of kerosene and heptane with volume ratio 50/50. All samples exhibit well-defined olivine patterns without any impurities. The CHN analysis of these samples showed that the carbon content gradually decreased from 37 to 8 wt.% after the addition of equal volumes of heptane and kerosene. Moreover, the sample prepared from pure heptane solvent contained only 3 wt.% carbon.

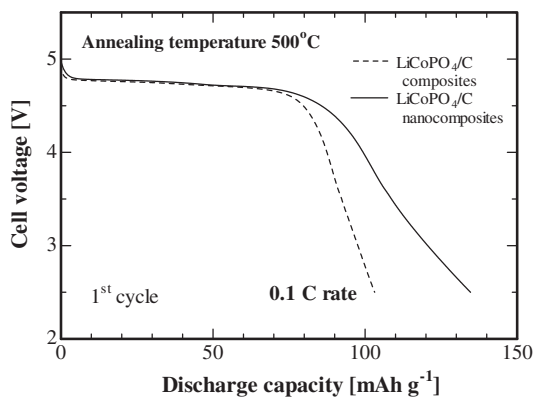


Fig. 7. Initial discharge curves of LiCoPO_4/C nanocomposites. Organic solvent: kerosene.

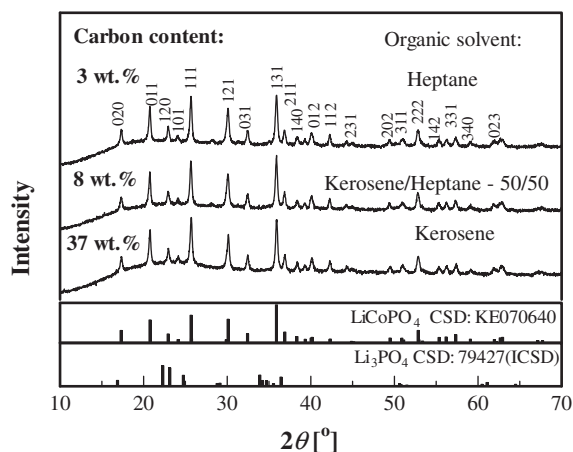


Fig. 8. XRD patterns of LiCoPO_4/C nanocomposites prepared from different organic solvents in emulsion.

Fig. 9a shows SEM images of the LiCoPO_4/C samples prepared from different organic solvents. The samples prepared from a mixture of kerosene and heptane and from pure heptane exhibited the same morphology as the sample prepared from pure kerosene. However, from the magnified SEM images, it was found that the geometric mean diameter of the LiCoPO_4 primary particles increases from 70 to 209 nm when the heptane in the oil phase is increased from 0 to 100%, as shown in Figs. 5b and 9b.

The distribution of carbon in the samples was investigated by TEM and EDS. The obtained results are shown in Fig. 10a and b for the samples prepared from a mixture of kerosene and heptane and from pure heptane, respectively. The TEM and EDS observations of the sample prepared from a mixture of kerosene and heptane revealed that the LiCoPO_4 nanoparticles were uniformly covered by a thin carbon layer with a thickness on the order of 10 nm, significantly less than that for the sample prepared from kerosene (Fig. 6). However, the TEM observation of the sample prepared from pure heptane showed that the carbon phase is located only in some parts of the surface of the LiCoPO_4 nanoparticles, and the majority of the surface is not covered by a carbon layer (Fig. 10b).

Fig. 11 shows the charge–discharge profiles of the LiCoPO_4/C nanocomposites prepared from different organic solvents. The LiCoPO_4/C nanocomposites prepared from a mixture of kerosene

and heptane exhibited two successive flat and wide potential plateaus at approximately 4.8 V and delivered an initial discharge capacity of 128 mAh g^{-1} , while the LiCoPO_4/C nanocomposites prepared from heptane delivered an initial discharge capacity of only 82 mAh g^{-1} . A LiCoPO_4/C nanocomposite electrode prepared from a mixture of kerosene and heptane is suitable for battery applications since it can provide a wide and flat potential plateau. Further electrochemical tests were conducted to determine the reason for the superior performance of LiCoPO_4/C nanocomposites prepared from a mixture of kerosene and heptanes.

Fig. 12 shows the CV curves of the LiCoPO_4/C nanocomposites prepared from different organic solvents. The intensity of the redox peaks for the sample prepared from a mixture of kerosene and heptane is much higher than those obtained for the samples prepared from kerosene and from heptane, indicating that the uniform thin layer of carbon is the origin of the improved electronic conductivity of the electrodes.

Fig. 13 shows the energy densities of the LiCoPO_4/C nanocomposites prepared from different organic solvents. The energy densities of the LiCoPO_4/C nanocomposites prepared from a mixture of kerosene and heptane and from kerosene and heptane were 595, 575 and 372 Wh kg^{-1} at a charge–discharge rate of 0.1 C, respectively. The LiCoPO_4/C nanocomposites prepared from a

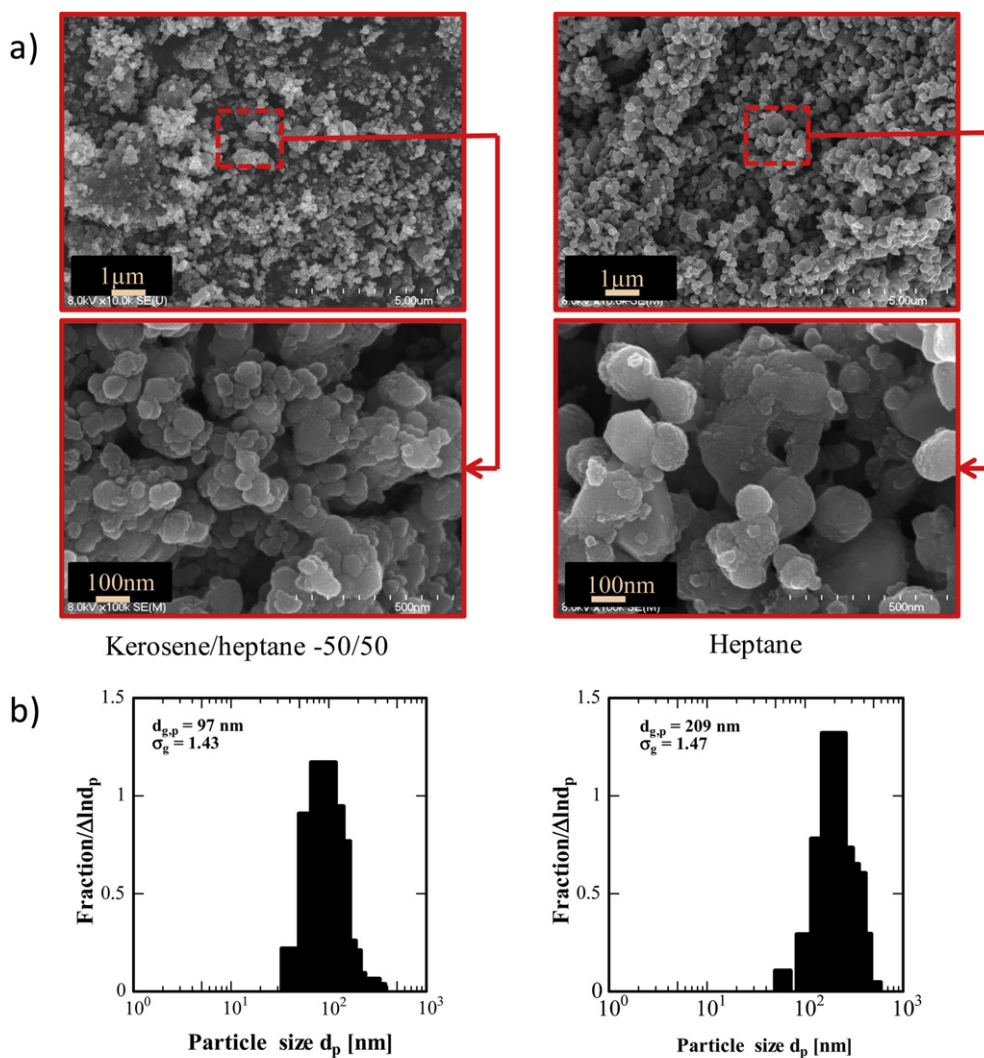


Fig. 9. SEM images (a) and particle size distribution (b) of LiCoPO_4/C nanocomposites prepared from different organic solvents in emulsion.

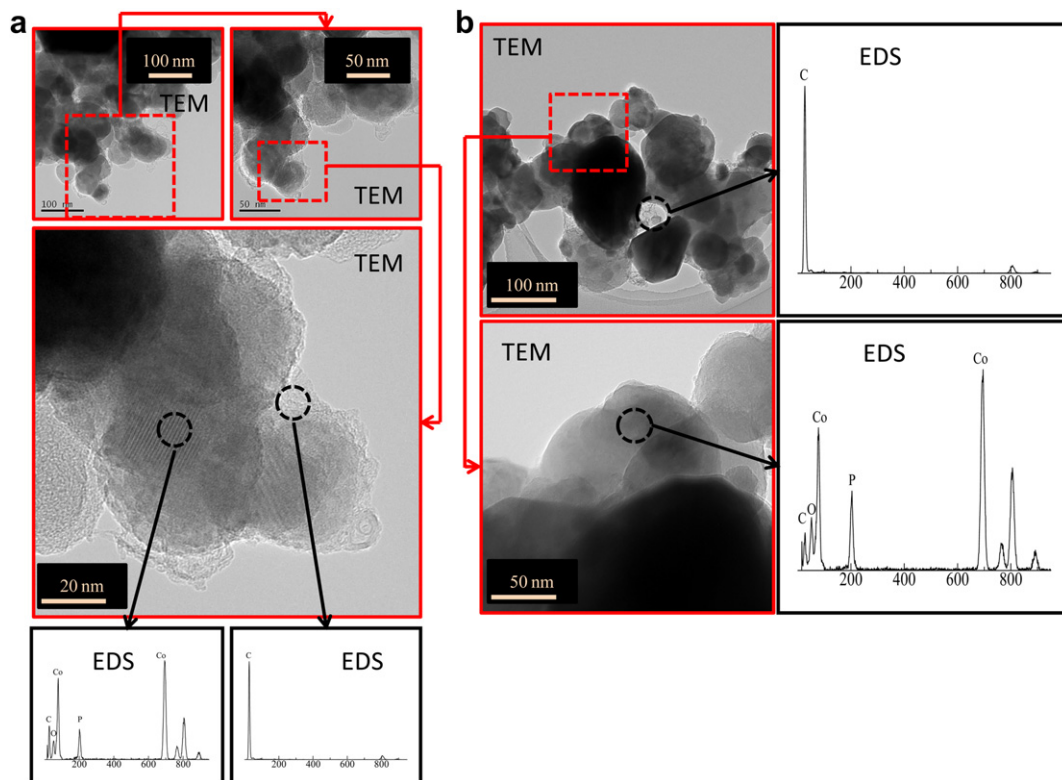


Fig. 10. TEM images with EDS spectra of LiCoPO_4/C nanocomposites. Organic solvent: kerosene/heptane with a volume ratio of 50/50 (a) and pure heptane (b).

mixture of kerosene and heptane exhibited the highest energy density at charge–discharge rates of 0.1, 0.5, 1 and 2 C.

Among the samples prepared from different organic solvents, the sample prepared from a mixture of kerosene and heptane had the best electrochemical performance. Thus, its cyclic performance was also investigated. Fig. 14 shows the cyclic performance of the LiCoPO_4/C nanocomposites tested at a charge–discharge rate of 0.1 C. The LiCoPO_4/C nanocomposites exhibited a good cyclic performance and delivered initial discharge capacity of 128 mAh g^{-1} , retaining 87% of the initial capacity after the 25th cycle, while the sample prepared from kerosene exhibited poor retention and delivered discharge capacity of 67 mAh g^{-1} after the 25th cycle, which is 50% of its initial discharge capacity.

The interfacial reaction resistance of the LiCoPO_4/C nanocomposite cell was further examined by electrochemical impedance spectroscopy. Fig. 15 shows Nyquist plots of LiCoPO_4/C nanocomposite cells prepared from the different organic solvents. Each profile comprised a depressed semicircle followed by a declining line. The depressed semicircles in the intermediate frequency region and the sloped lines in the low-frequency region correspond to the charge transfer resistance at the electrode/electrolyte interface and the Warburg impedance associated with lithium ion diffusion in the cathode material, respectively. The LiCoPO_4/C nanocomposite electrode prepared from a mixture of kerosene and heptane exhibited the smallest depressed semicircle, indicating the smallest charge transfer resistance among the three types of electrode. It is well known that the smaller the resistance of the electrode material, the higher the electronic conductivity of

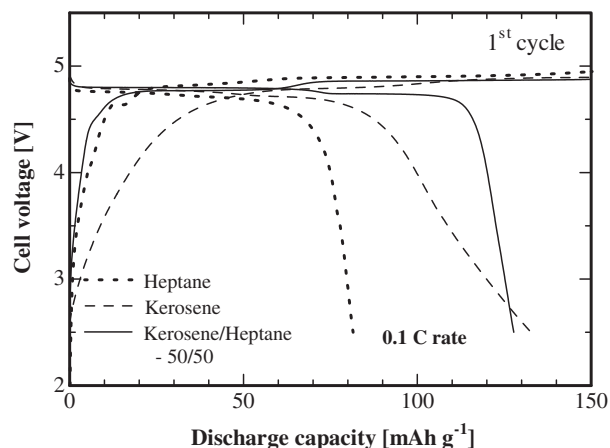


Fig. 11. Initial charge and discharge curves of the cells using LiCoPO_4/C nanocomposites prepared from different organic solvents at a charge–discharge rate of 0.1 C.

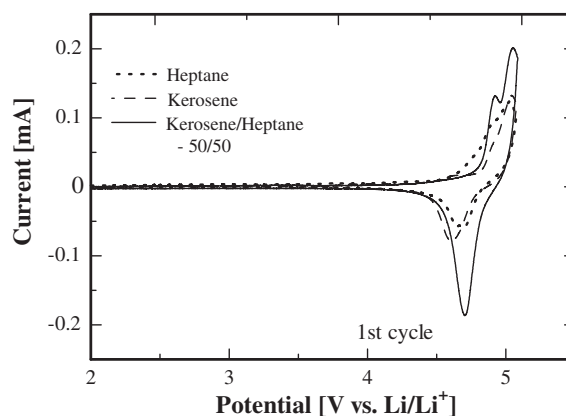


Fig. 12. Cyclic voltammogram of the cells using LiCoPO_4/C nanocomposites prepared from different organic solvents.

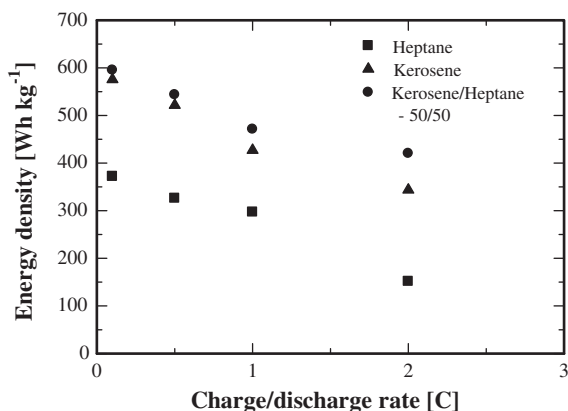


Fig. 13. Energy density of the cells using LiCoPO₄/C nanocomposites prepared from different organic solvents at various charge–discharge rates.

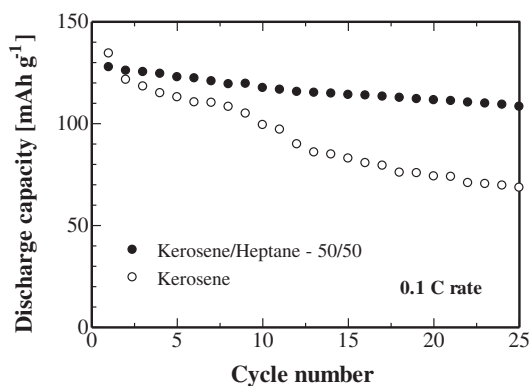


Fig. 14. Cycle performance of the cells using LiCoPO₄/C nanocomposites prepared from different organic solvents at a charge–discharge rate of 0.1 C.

the electrode. Therefore, we concluded that the superior electrochemical performance of the LiCoPO₄/C nanocomposite electrode can be attributed to the smaller primary particle size of LiCoPO₄ and the thinner carbon layer formed on the surface of the LiCoPO₄ primary particles. Dominko et al. [24] also reported the importance

of the distribution of a sufficient amount of carbon on the surface of LiFePO₄ particles.

5. Conclusions

LiCoPO₄/C composites were successfully prepared by emulsion drip combustion at 600 °C in a fluidized bed reactor followed by heat treatment at 500 °C in a N₂ + 3% H₂ atmosphere. The cell containing LiCoPO₄/C composites exhibited a discharge capacity of 103 mAh g^{−1} at a charge–discharge rate of 0.1 C, which corresponds to 62% of the theoretical capacity (167 mAh g^{−1}). The combination of emulsion drip combustion at 600 °C and wet ball-milling followed by heat treatment at 500 °C was performed for the preparation of LiCoPO₄/C nanocomposites. The obtained material consisted of agglomerates of the LiCoPO₄ primary particles with a geometric mean diameter of 70 nm, which were covered by a thick layer of amorphous carbon. The cell containing LiCoPO₄/C nanocomposites exhibited superior electrochemical properties to containing LiCoPO₄/C composites, delivering a discharge capacity of 134 mAh g^{−1} at a charge–discharge rate of 0.1 C. However, the discharge profile of the LiCoPO₄/C nanocomposites has a long tail, which may be due to the limited Li-ion diffusion caused by the thicker carbon layer that formed on the LiCoPO₄ particles. The electrochemical properties of the LiCoPO₄/C nanocomposites were improved by decreasing of the carbon content in the final samples, which was achieved by mixing kerosene with heptane, a lighter hydrocarbon. The LiCoPO₄/C nanocomposites prepared from a mixture of kerosene and heptane with equal volumes consisted of agglomerates of the primary particles with a geometric mean diameter of 97 nm, which were covered by a thin layer of amorphous carbon with thickness on the order of 10 nm. Furthermore, they delivered a high initial discharge capacity and high energy density at a charge–discharge rate of 0.1 C which were 128 mAh g^{−1} and 595 Wh kg^{−1}, respectively. The LiCoPO₄/C nanocomposites exhibited reasonable cyclability, retaining 87% of the initial discharge capacity after 25 cycles.

Acknowledgements

The authors are grateful to Mr. A. Hori and Mr. J. Koki, staff members of the Center for Advanced Materials Analysis (Tokyo Institute of Technology, Japan) for the TEM observation of the samples.

References

- [1] A.K. Padhi, K.S. Nanjundaswamy, J.B. Goodenough, *J. Electrochem. Soc.* 144 (1997) 1188–1194.
- [2] K. Amine, H. Yasuda, M. Yamachi, *Electrochem. Solid State Lett.* 3 (2000) 178–179.
- [3] J. Wolfenstine, U. Lee, B. Poesse, J.L. Allen, *J. Power Sources* 144 (2005) 226–230.
- [4] K. Tadanaga, F. Mizuno, A. Hayashi, T. Minami, M. Tatsumisago, *Electrochemistry* 71 (2003) 1192–1195.
- [5] J.M. Lloris, C.P. Vicente, J.L. Tirado, *Electrochem. Solid State Lett.* 5 (2002) A234–A237.
- [6] M.E. Rabanal, M.C. Gutierrez, F. Garcia-Alvarado, E.C. Gonzalo, M.E. Arroyo-de Dompablo, *J. Power Sources* 160 (2006) 523–528.
- [7] F. Wang, J. Yang, Y. NuLi, J. Wang, *J. Power Sources* 195 (2010) 6884–6887.
- [8] J.L. Allen, T.R. Jow, J. Wolfenstine, *J. Power Sources* 196 (2011) 8656–8661.
- [9] D.-W. Han, Y.-M. Kang, R.-Z. Yin, M.-S. Song, H.-S. Kwon, *Electrochem. Commun.* 11 (2009) 137–140.
- [10] D. Shanmukaraj, R. Murugan, *Ionics* 10 (2004) 88–92.
- [11] I.C. Jang, H.H. Lim, S.B. Lee, K. Karthikeyan, V. Aravindan, K.S. Kang, W.S. Yoon, W.I. Cho, Y.S. Lee, *J. Alloys Compd.* 497 (2010) 321–324.
- [12] A. Eftekhari, *J. Electrochem. Soc.* 151 (2004) A1456–A1460.
- [13] D. Gangulibabu, N. Bhuvaneshwari, N. Kalaiselvi, P. Jayaprakash, J. Periasamy, *J. Sol-Gel Sci. Tech.* 49 (2009) 137–144.
- [14] J. Wolfenstine, J. Read, J.L. Allen, *J. Power Sources* 163 (2007) 1070–1073.
- [15] H.H. Li, J. Jin, J.P. Wei, Z. Zhou, J. Yan, *Electrochem. Commun.* 11 (2009) 95–98.

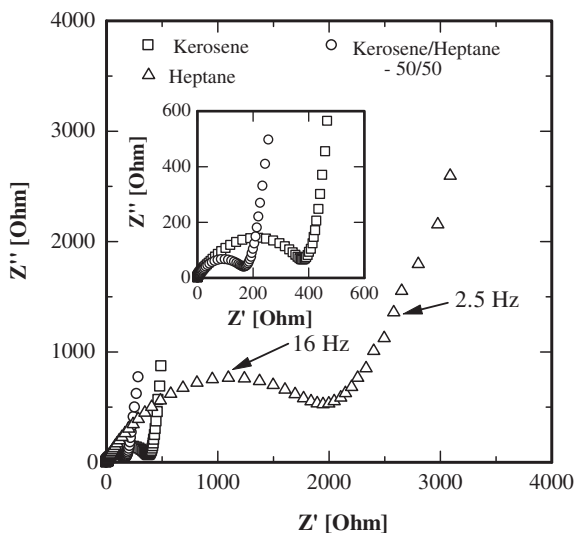


Fig. 15. Nyquist plots of the cells using the LiCoPO₄/C nanocomposites prepared from different organic solvents.

- [16] A.V. Murugan, T. Muraliganth, A. Manthiram, *J. Electrochem. Soc.* 156 (2009) A79–A83.
- [17] R. Sharabi, E. Markevich, V. Borgel, G. Salitra, G. Gershtinsky, D. Aurbach, G. Semrau, M.A. Schmidt, N. Schall, C. Stinner, *J. Power Sources* 203 (2012) 109–114.
- [18] R. Vasanthi, D. Kalpana, N.G. Renganathan, *J. Solid State Electrochem.* 12 (2008) 961–969.
- [19] J. Yang, J.J. Xu, *J. Electrochem. Soc.* 153 (2006) A716–A723.
- [20] F. Wang, J. Yang, Y. Nuli, J. Wang, *J. Power Sources* 196 (2011) 4806–4810.
- [21] R. Tussupbayev, T. Shokanbay, Z. Bakenov, I. Taniguchi, *J. Chem. Eng. Jpn.* 44 (2011) 179–186.
- [22] C.Y. Wen, Y.H. Yu, *AIChE* 12 (1966) 610–612.
- [23] N.N. Bramnik, K.G. Bramnik, C. Baehtz, H. Ehrenberg, *J. Power Sources* 145 (2005) 74–81.
- [24] R. Dominko, M. Gaberscek, J. Drofenik, M. Bele, S. Pejovnik, J. Jamnik, *J. Power Sources* 119–121 (2003) 770–773.